IJCRT.ORG ISSN : 2320-2882

INTERNATIONAL JOURNAL OF CREATIVE RESEARCH THOUGHTS (IJCRT)

An International Open Access, Peer-reviewed, Refereed Journal

DESIGN AND ANALYISIS OF AN OLOID-SHAPED MICROSTRIP PATCH ANTENNA FOR S-BAND RADAR SYSTEM

Mrs.N.Srividhya, Satyanarayanan S, Sharmilan M, Varun P ,Vishva R

UG Students

Department of Electronics and Communication Engineering,

K. Ramakrishnan College of Engineering, Trichy, Tamil Nadu, India

Abstract: *Microstrip patch antennas occupy a central role in contemporary wireless communication systems, owing to their thin profile, low mass, economical production, and ease of integration with printed circuit boards. This paper describes the development and electromagnetic simulation of a microstrip patch antenna designed in the shape of an oloid, wherein circular and elliptical boundaries are geometrically merged to produce a smoothly curved, non-conventional radiating element. The antenna is fabricated on a commonly used FR-4 substrate with a dielectric constant of 4.4 and a thickness of 1.6 mm, and its performance is analyzed using CST Studio Suite 2025. The simulation results indicate a resonant frequency of 3.8 GHz, achieving a reflection coefficient (S11) of −13.33 dB and a VSWR of 1.55, which fall within acceptable performance limits. Additionally, far-field analysis at 2 GHz reveals a bidirectional radiation pattern, with a peak gain of 0.384 dBi, a main beam directed at 62°, and a 3 dB beamwidth of 124°. Surface current analysis verifies concentrated excitation near the feed point, confirming proper antenna operation. The proposed design is identified as a viable candidate for integration in compact wireless devices.*

Keywords— *Oloid-Shaped Patch Antenna; FR-4 Substrate; CST Studio Suite; S11; VSWR; Far-Field Radiation; Surface Current; Wireless Communication.*

I. INTRODUCTION

Rapid advancements in wireless technology have generated a sustained demand for antenna systems that are compact, efficient, and compatible with modern fabrication techniques. Microstrip patch antennas satisfy these requirements through their planar architecture, which allows direct integration with the host circuit board without the mechanical complexity associated with traditional antenna structures. Their low weight and low profile make them particularly attractive for portable and wearable wireless devices.

A typical microstrip patch antenna is made up of a metal radiating patch placed on one side of a dielectric substrate, while the other side is covered with a continuous conducting ground plane. While rectangular and circular patch geometries are widely adopted in practice, both configurations tend to exhibit restricted impedance bandwidth and moderate radiation efficiency, which impose limitations on their applicability in wideband or high-performance scenarios.

A well-established strategy for overcoming these limitations is the modification of the patch boundary geometry. Altering the shape of the radiating element directly influences the distribution of electromagnetic surface currents across the patch, which in turn determines resonant frequency behaviour, impedance matching characteristics, and far-field radiation properties. Using unconventional shapes can increase the antenna's effective electrical path without increasing its physical size, which helps it achieve resonance at lower frequencies while staying compact.

Motivated by these considerations, this paper proposes an oloid-inspired patch geometry. The oloid is a mathematical solid whose surface is generated by two intersecting circles of equal radius, positioned perpendicular to each other. In the two-dimensional representation adopted for this design, the patch boundary is formed by the smooth intersection of a circular arc and an elliptical curve, producing a continuous, asymmetry-free edge profile. This geometry is hypothesised to promote a more uniform surface current distribution and reduce impedance discontinuities at the patch boundary.

The antenna is built using an FR-4 substrate and its performance is analyzed through simulations carried out in CST Studio Suite 2025. The paper details the design rationale, geometric parameters, simulation methodology, and a comprehensive analysis of the resulting S11, VSWR, far-field radiation, and surface current characteristics.

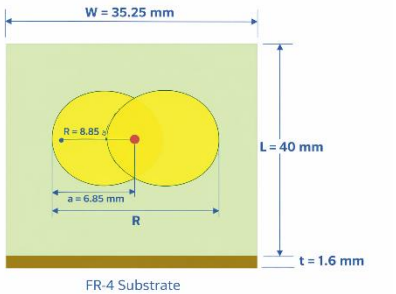

Fig. 1. Proposed oloid-shaped patch antenna — geometry view

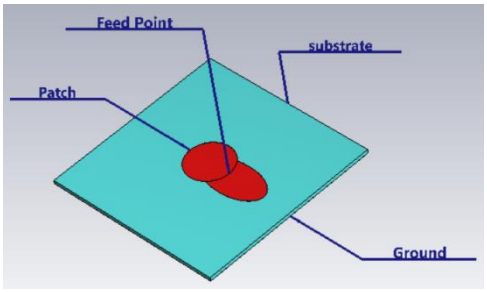

Fig. 2. Three-dimensional perspective of the antenna structure

II. ANTENNA DESIGN

The proposed antenna follows the classical three-layer microstrip configuration: a bottom ground plane, an intermediate dielectric substrate, and an upper radiating patch. Each layer is described below.

A. Substrate

FR-4 glass-epoxy is chosen as the substrate material because it is easily available, affordable, and has well-known dielectric characteristics. It has a relative permittivity of 4.4 and a loss tangent of about 0.02, and a thickness of 1.6 mm is used for the design. representing the most commonly available standard thickness in PCB manufacturing. The lateral dimensions of the substrate are set at 40 mm × 40 mm, chosen to accommodate the patch geometry while providing adequate ground plane extent.

B. Ground Plane

A full-coverage copper ground plane, dimensionally identical to the substrate (40 mm × 40 mm), is placed on the lower face. The continuous ground plane provides a well-defined electromagnetic reference plane and directs radiated energy upward from the patch surface, improving the forward gain of the antenna. The copper layer thickness is 0.035 mm, consistent with standard one-ounce copper PCB cladding.

C. Oloid-Shaped Radiating Patch

The radiating patch constitutes the primary novel contribution of this design. The boundary inspired by the oloid shape is created by merging a circle with a 10 mm radius and an ellipse defined by a semi-major axis of 15 mm and a semi-minor axis of 8 mm. The boundary curves are blended smoothly to eliminate sharp corners, producing a continuous edge profile without discontinuities.

This geometry extends the effective electrical circumference of the patch relative to a simple circular patch of the same enclosed area. The extended and curved boundary modifies the distribution of induced surface currents, creating longer and more varied current paths that can support improved impedance matching. The smooth curvature also suppresses fringe field discontinuities that commonly arise at the sharp corners of rectangular patches, reducing unwanted cross-polarisation radiation.

D. Feeding Method

A 50-ohm microstrip feed line is used to energize the antenna. In the CST simulation setup, a discrete port is placed between the end of the feed line and the ground plane, with port impedance fixed at 50 Ω. The feed line position is optimised iteratively to minimise the S11 at the target resonant frequency of 3.8 GHz, ensuring efficient energy coupling from the source into the radiating element.

Table 1: Proposed Antenna Design Parameters

Parameter	Value
Substrate Material	FR-4
Relative Permittivity (εr)	4.4
Loss Tangent	0.02
Substrate Size	40 × 40 mm
Substrate Thickness	1.6 mm
Ground Plane Size	40 × 40 mm
Copper Layer Thickness	0.035 mm
Circular Patch Radius	10 mm
Ellipse Semi-Major Axis	15 mm
Ellipse Semi-Minor Axis	8 mm
Feed Line Impedance	50 Ω
Target Resonant Frequency	3.8 GHz

III. DESIGN PROCEDURE

The antenna was constructed and analysed in CST Studio Suite 2025 following a sequential four-stage procedure.

Stage 1: Substrate and Ground Plane Definition

The FR-4 substrate block (40 × 40 × 1.6 mm) is defined first with material properties εr = 4.4 and tan δ = 0.02. A Perfect Electric Conductor (PEC) layer representing the ground plane is bonded to the bottom face of the substrate.

Stage 2: Oloid Patch Construction

The circular boundary (r = 10 mm) and the elliptical boundary (a = 15 mm, b = 8 mm) are drawn on the top face of the substrate. A Boolean union operation with edge smoothing is applied to merge the two curves into a single continuous closed boundary, which is then extruded as a 0.035 mm copper solid to form the radiating patch.

Fig. 3. Sequential construction stages of the proposed antenna in CST

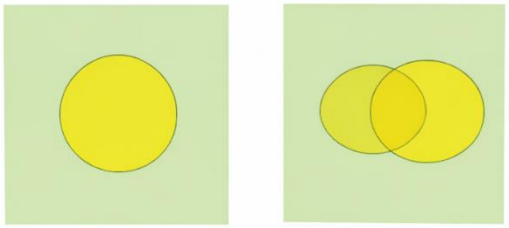

Stage 3: Feed Line and Port Assignment

A 50-ohm microstrip feed line is extended from the edge of the substrate to the patch, and a discrete port is defined at its base to link the feed conductor with the ground plane. The feed point location along the patch boundary is parametrically optimised to achieve minimum S11 at 3.8 GHz.

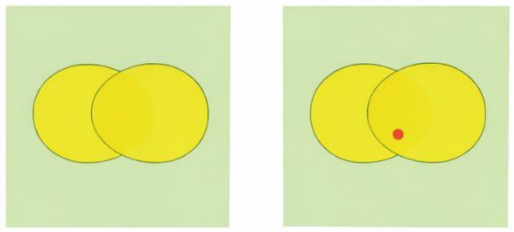

Stage 4: Simulation Configuration

Frequency domain simulation is performed over the range of 2–10 GHz. Open boundary conditions with additional free-space padding of a quarter wavelength are applied on all six faces of the simulation domain to accurately model far-field radiation conditions. Adaptive tetrahedral mesh refinement is enabled, with enhanced mesh density applied at the patch edges and feed transition to capture high-field-gradient regions accurately. Field monitors for electric field, surface current, and far-field patterns are activated at 2 GHz and 3.8 GHz.

IV. RESULTS AND DISCUSSION

The proposed oloid-shaped antenna was comprehensively evaluated through CST Studio Suite 2025 simulation. The following subsections present and interpret the four primary performance metrics: reflection coefficient, VSWR, far-field radiation pattern, and surface current distribution.

A. Reflection Coefficient (S11)

The parameter S11 represents how much of the input signal is reflected back from the antenna port compared to the power supplied, and it is usually measured in decibels. In general, an S11 value lower than −10 dB is considered acceptable for good antenna performance, since it indicates that over 90% of the input power is effectively radiated instead of being reflected back toward the source.

Fig. 4 presents the S11 magnitude as a function of frequency over the range 2–10 GHz. The plot displays a clear and sharp dip in the S11 curve at 3.8 GHz, where it reaches a minimum value of −13.33 dB. This pronounced drop indicates strong resonance at the desired frequency and suggests that the oloid-shaped boundary helps achieve effective coupling between the feed line and the radiating patch at 3.8 GHz.The resonance profile is symmetric and well-separated from the

surrounding out-of-band response, demonstrating stable single-band operation.

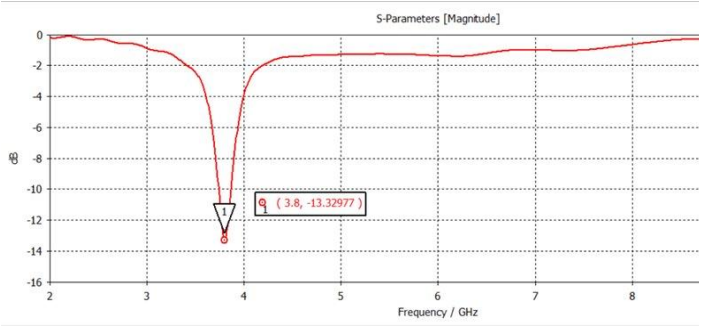

Fig. 4. Simulated S11 (return loss) vs. frequency — resonance at 3.8 GHz, S11 = −13.33 dB

Table 2: Reflection Coefficient Summary

Resonant Freq. (GHz)	S11 (dB)	Status
3.8	−13.33	Pass (< −10 dB)

B. Voltage Standing Wave Ratio (VSWR)

The Voltage Standing Wave Ratio (VSWR) indicates how well the antenna's impedance matches that of the transmission line.A VSWR of 1 represents an ideal matched condition with zero reflection, while the practical upper limit for acceptable antenna operation is conventionally set at VSWR ≤ 2, which corresponds to a reflected power fraction below 11%.

The VSWR characteristic of the proposed antenna across 2–10 GHz is displayed in Fig. 5. A global minimum VSWR of 1.55 is recorded at 3.8 GHz, consistent with the resonance identified in the S11 analysis. This value falls well within the ≤ 2 acceptance criterion, confirming efficient power delivery to the antenna at resonance. Outside the resonant band — particularly below 3 GHz and above 8 GHz — the VSWR rises substantially, reflecting the expected single-band character of the antenna. These elevated values in non-resonant regions are an anticipated feature of the design and do not constitute a performance deficiency for targeted single-band operation.

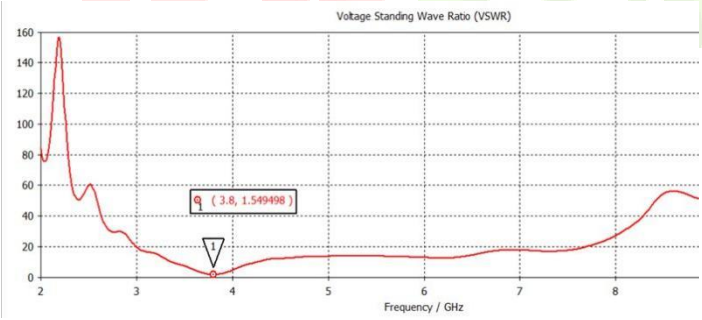

Fig. 5. Simulated VSWR vs. frequency — minimum VSWR = 1.55 at 3.8 GHz

Table 3: VSWR Summary

Resonant Freq. (GHz)	VSWR	Status
3.8	1.55	Pass (< 2.0)

C. Surface Current Distribution

Fig. 6 illustrates the distribution of surface current vectors over the antenna at its operating frequency The colour map transitions from blue (low current density) through green and yellow to red-orange (high current density), providing a clear spatial picture of the current flow mechanism.

The current distribution reveals a well-defined concentration of high-density current near the feed point and across the central region of the oloid patch, particularly along the circular portion of the patch boundary. This indicates strong electromagnetic coupling in the feed vicinity and confirms that the patch is efficiently excited at the operating frequency. The current vectors radiate outward from the high-density core toward the elliptical edges, producing a distributed and progressive current pattern across the entire patch surface.

The smooth and continuous nature of the oloid boundary is reflected in the gradual transition of current density from the central high-intensity region toward the patch periphery, without abrupt discontinuities. This uniformity in current flow is a direct consequence of the absence of sharp corners in the geometry, and it contributes to the stable impedance matching observed in the S11 and VSWR results. The ground plane region exhibits significantly lower current intensity, confirming minimal energy loss in the ground structure.

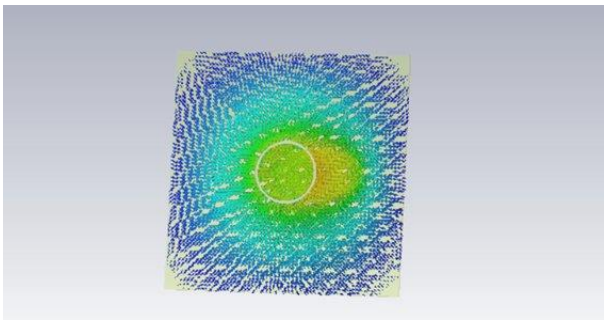

Fig. 6. Simulated surface current distribution at f = 3.8 GHz

D. Far-Field Radiation Pattern

At a frequency of 2 GHz, the far-field directivity at Phi = 90° is analyzed and shown as a polar plot in Fig. 7. This pattern illustrates how the radiated power is distributed across different angles in the elevation plane, offering a clear view of the antenna's directional characteristics.

The simulated far-field pattern exhibits a clear bidirectional radiation characteristic, with two approximately symmetric major lobes oriented broadly toward the upper and lower hemispheres of the plot. The main lobe magnitude is 0.384 dBi, indicating a near-omnidirectional radiation behaviour with low directional preference in this plane. The main lobe direction is recorded at 62° from the reference axis, and the angular width at the 3 dB points spans 124°, confirming exceptionally broad beam coverage.

The wide 3 dB beamwidth of 124° makes the antenna well suited for applications that require broad spatial coverage without beam steering or array processing. The bidirectional pattern is consistent with the expected radiation behaviour of a planar patch antenna in the absence of a highly reflective ground structure. A radiation null is observed near 180°, representing a characteristic feature of the symmetric bidirectional pattern and confirming the integrity of the far-field computation.

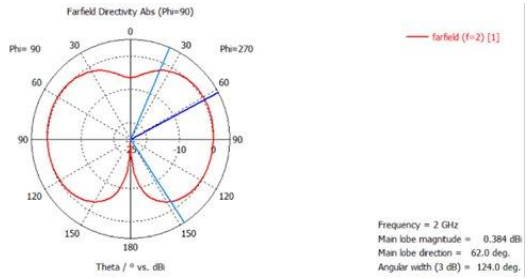

Fig. 7. Simulated far-field directivity pattern (Phi = 90°) at f = 2 GHz — main lobe = 0.384 dBi, direction = 62°, 3 dB BW = 124°

Table 4: Comprehensive Performance Summary of the Proposed Antenna

Parameter	Achieved Value
Resonant Frequency	3.8 GHz
Minimum S11	−13.33 dB
VSWR at Resonance	1.55
Main Lobe Magnitude	0.384 dBi
Main Lobe Direction	62°
3 dB Beamwidth	124°
Radiation Pattern Type	Bidirectional
Peak Surface Current	Concentrated at feed & patch centre

Substrate	FR-4, εr = 4.4, h = 1.6 mm
Simulation Tool	CST Studio Suite 2025

V. CONCLUSION

This paper has presented the design, construction, and electromagnetic simulation of an oloid-shaped microstrip patch antenna fabricated on an FR-4 dielectric substrate for wireless communication applications. The antenna was fully modelled and analysed within CST Studio Suite 2025, with simulation spanning 2–10 GHz.

The reflection coefficient analysis confirmed resonance at 3.8 GHz with a minimum S11 of −13.33 dB, satisfying the −10 dB operational threshold and indicating efficient power radiation at the design frequency. The corresponding VSWR of 1.55 at resonance confirms strong impedance matching between the 50 Ω feed network and the antenna element, consistent with less than 4% reflected power at the input port.

Surface current analysis revealed a well-defined concentration of current near the feed region and along the central oloid patch area, with smooth current gradients extending toward the elliptical periphery — a direct consequence of the corner-free, continuously curved patch boundary. The far-field radiation pattern at 2 GHz demonstrated bidirectional behaviour with a broad 3 dB beamwidth of 124° and a main lobe magnitude of 0.384 dBi, indicating broad angular coverage suited for wireless systems that do not require narrow directional beams.

The proposed oloid geometry demonstrates that non-conventional mathematically derived patch shapes can yield practically useful and fabrication-compatible antenna designs. The achieved performance parameters position the antenna as a suitable candidate for deployment in compact wireless communication systems, WLAN, and S-band microwave applications. Future research may investigate array configurations of the proposed element to enhance gain, as well as the use of lower-loss substrates such as Rogers RT/duroid to improve radiation efficiency and bandwidth.

VI. ACKNOWLEDGEMENT

The authors sincerely acknowledge the guidance and support of the faculty members of the Department of Electronics and Communication Engineering, K. Ramakrishnan College of Engineering, Trichy, throughout this research. The authors also thank the department for providing access to CST Studio Suite 2025 for electromagnetic simulation. The constructive feedback received during the preparation of this work is gratefully recognised.

REFERENCES

[1] C. A. Balanis, Antenna Theory: Analysis and Design, 4th ed. Hoboken, NJ, USA: Wiley, 2016.

[2] D. M. Pozar, Microwave Engineering, 4th ed. Hoboken, NJ, USA: Wiley, 2012.

[3] R. Garg, P. Bhartia, I. Bahl, and A. Ittipiboon, Microstrip Antenna Design Handbook. Boston, MA, USA: Artech House, 2001.

[4] K. L. Wong, Compact and Broadband Microstrip Antennas. New York, NY, USA: Wiley, 2002.

[5] T. S. Rappaport, Wireless Communications: Principles and Practice, 2nd ed. Upper Saddle River, NJ, USA: Prentice Hall, 2002.

[6] J. Volakis, C. Chen, and K. Fujimoto, Small Antennas: Miniaturization Techniques and Applications. New York, NY, USA: McGraw-Hill, 2010.

[7] S. J. Orfanidis, Electromagnetic Waves and Antennas. Rutgers University, 2016. [Online]. Available: https://www.ece.rutgers.edu/~orfanidi/ewa/

[8] CST Studio Suite 2025, Computer Simulation Technology GmbH, Darmstadt, Germany. [Online]. Available: https://www.cst.com

[9] R. Waterhouse, Printed Antennas for Wireless Communications. Hoboken, NJ, USA: Wiley, 2007.

[10] H. Wong and K. M. Luk, Microstrip Antennas: Design Handbook. London, U.K.: Imperial College Press, 2012.

[11] A. A. Deshmukh and K. P. Ray, "Compact broadband microstrip antennas," IEEE Antennas Propag. Mag., vol. 51, no. 2, pp. 33–46, Apr. 2009.

[12] I. J. Bahl and P. Trivedi, "A designer's guide to microstrip line," Microwaves, vol. 16, pp. 174–182, May 1977.